Available online at www.sciencedirect.com
SCIENCE DIRECT®
ELSEVIER
Nuclear Instruments and Methods in Physics Research B 225 (2004) 72–77
NIM B
Beam Interactions with Materials & Atoms
www.elsevier.com/locate/nimb

Non-equilibrium emission of secondary ions from BeO films sputtered by swift gold ions

K. Czerski [a,*], G. Schiwietz [a], M. Roth [a], F. Staufenbiel [a], P. Grande [b], S.R. Bhattacharyya [c]

[a] *Hahn-Meitner-Institut, Bereich Strukturforschung, Glienicker Str. 100, D-14109 Berlin, Germany*
[b] *Instituto de Fisica, Universidade Federal do Rio Grande do Sul, Porto Alegre, Brazil*
[c] *Surface Physics Division, Saha Institute of Nuclear Physics, Kolkata, India*

Received 13 January 2004; received in revised form 25 May 2004

Abstract

Electronic sputtering of thin BeO films induced by Au^{26+} and Au^{41+} ions has been studied at the beam energy of 1.8 MeV/u and compared to the experimental results obtained under nuclear sputtering conditions. Energy spectra and angular distributions of secondary positive ions (Be^+ and O^+) as well as negative ions (O^-, BeO^- and BeO_2^-) have been measured using a quadrupole mass spectrometer. Contrary to the nuclear sputtering, the data for swift heavy-ion irradiation show significant differences in the sputtering process between positive and negative ions. Whereas the angular distribution of the negative ions is nearly isotropic, the emission of the positive ions is strongly anisotropic and enhanced at the directions corresponding to the incident half-space. Additionally, an enhanced high-energy contribution in the energy spectra of positive ions can be observed. The electronic sputtering process of positive ions cannot be explained in the frame of the simple thermal spike model assuming a thermal equilibrium within the ion-track in the target material. An application of the gas-flow model describing an adiabatic expansion of high temperature plasma outside the target has been proposed.

PACS: 79.20.Rf; 61.80.Jh; 78.55.Fv
Keywords: Sputtering by swift heavy ions; Nuclear sputtering; Non-equilibrium effects; Emission of secondary ions

1. Introduction

Emission of secondary particles from target surfaces irradiated by fast heavy ions (a few MeV/u) is usually dominated by the electronic sputtering. Contrary to the low-energy nuclear sputtering which is directly energized by a cascade of screened nuclear collisions, the fast ions create first a cylindrical track of ionization and electronic excitation in the target. Only at the second step the electronic energy is released into atomic modes of motion and the emission of secondary ions as well as neutral particles can occur. The electronic

* Corresponding author. Tel.: +49-30-8062-2338; fax: +49-30-8062-2293.
E-mail address: czerski@hmi.de (K. Czerski).

0168-583X/$ - see front matter © 2004 Elsevier B.V. All rights reserved.
doi:10.1016/j.nimb.2004.06.001

sputtering process is usually described in the frame of the thermal spike model for both metallic [1] and insulating [2] materials. The model assumes the electron–phonon coupling as the energy transfer mechanism leading to a local thermal equilibrium for the spatio-temporal evolution of the ion track. Thus, the temperature at the target surface determines both the Maxwell–Boltzmann energy distribution of emitted particles and the total sputtering yield. The originally isotropic angular distribution is only modified by the surface binding potential leading to the cosine-type dependence on the emission angle.

Recently [3], a strong enhancement of neutral particle emission in the normal direction with respect to the target surface has been observed for sputtering of LiF under bombardment by swift heavy ions. The origin of this non-equilibrium contribution to the electronic sputtering remains unclear. In this work, we present an evidence for the anisotropic electronic sputtering of thin BeO films. Contrary to [3], we observe the anisotropic emission of charged particles. For comparison, angular distributions of secondary ions emitted from the same target but under nuclear sputtering conditions will be presented too.

2. Experimental set-up

The sputtering of BeO films were studied using a quadrupole mass spectrometer (Hiden HAL IV EQS-System) operated under ultra high vacuum conditions. The spectrometer simultaneously enabled very good mass resolution (<0.1 amu) and measurements of energy spectra of charged particles emitted in the energy range 0–100 eV with a nominal energy resolution of 0.5 eV.

The BeO films were produced by implanting 500 eV oxygen ions into an atomically clean beryllium target in the preparation chamber. The BeO layer checked by means of Auger-electron spectroscopy, showed the same electronic band structure as the natural oxide. In Fig. 1 a series of electron induced Auger spectra taken after different implantation times – beginning with a clean metallic target and finished after 40 min – are presented. The spectra can be understood as a

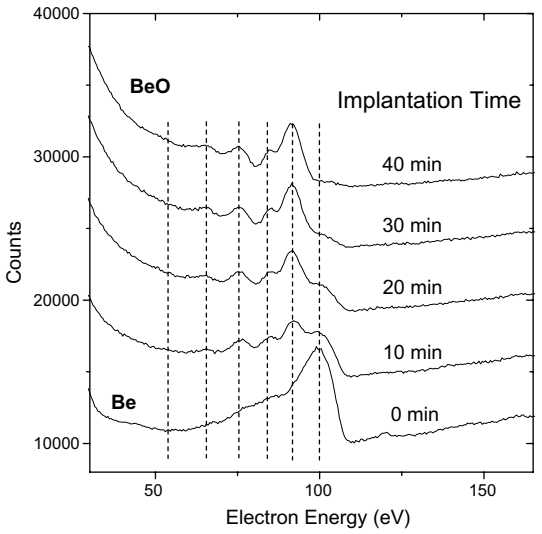

Fig. 1. Auger-electron spectra at different oxygen implantation times (500 eV O^+ ions at a flux of about 10^{12} ions/cm^2/s) induced by 2.7 keV electron irradiation. Vertical dashed lines mark the characteristic metallic Be Auger line at the energy 100 eV and the multi-peak structure of BeO shifted by 10 eV towards lower energies.

superposition of two structures changing their intensity in the course of implantation. One structure is a single line with a maximum at the energy of 100 eV corresponding to the KVV-Auger transition in metallic Be. The second one at lower energies corresponds to natural BeO and has a characteristic multi-peak fine structure. After 40 min of oxygen implantation, the metallic Be line was disappeared, and the Be target surface was fully oxidized. The same Auger spectrum can be obtained for the chemisorption of oxygen by Be targets in an oxygen atmosphere (see Fig. 2). During the beam time the target was implanted several times in order to keep the BeO thickness constant.

After implantation the target was moved to the main chamber (for details see [4]) by a manipulator which also allowed for rotation of the target around two perpendicular axes. Since the mass spectrometer was mounted at the target chamber at the fixed backward angle of 135° with respect to the beam direction, the target rotation provided the only possibility for a study of a sputtering angular distribution. The beam of Au^{26+} ions at an

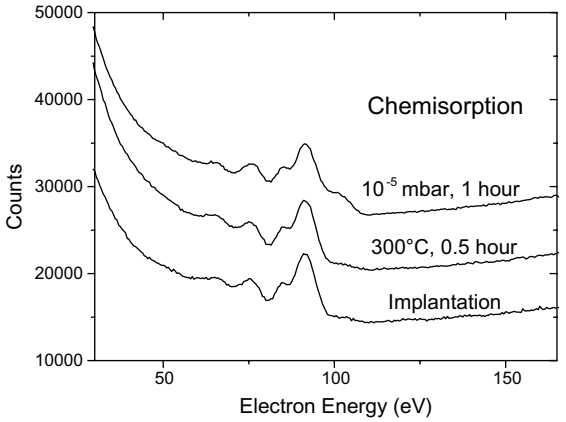

Fig. 2. Auger-electron spectra obtained after the oxygen chemisorption by a Be target in an oxygen atmosphere (upper curve), followed by the target heating at about 300 °C. The lowest curve corresponds to 40 min of implantation at room temperature (see Fig. 1).

energy per nucleon of 1.8 MeV/u was delivered by the heavy-ion cyclotron of the Hahn-Meitner-Institut Berlin. Applying a thin Al stripper foil (100 μg/cm^2) located in front of the target chamber, the charge state of projectiles could be increased to an average of Au^{41+}. Additionally, nuclear sputtering was investigated using a 2.5 keV Ar^+ beam from an ion gun placed at the target chamber. Energy spectra of positive (Be^+, O^+) and negative (O^-, BeO^-, BeO_2^-) ions were measured for different incident angles α and emission angles β (here defined with respect to the normal direction of the target surface). Both incidence and emission directions together with the target normal lay in the same plane (sputtering plane). The plane perpendicular to the sputtering plane involving the target normal divided the entire space into two half-spaces, whereby the half-space involving the incidence direction is denoted as the incidence half-space. Due to the fixed position of the mass spectrometer, the incident angle was related to the emission angle β as follows: $\beta - \alpha = 45°$ for the electronic sputtering, and $\beta - \alpha = 67.5°$ in the case of the nuclear sputtering.

Exemplary energy spectra of Be^+ and O^- ions taken for Au^{26+} and Au^{41+} projectiles are presented in Fig. 3. Because of contact potentials, the zero point of the energy scale is uncertain by about

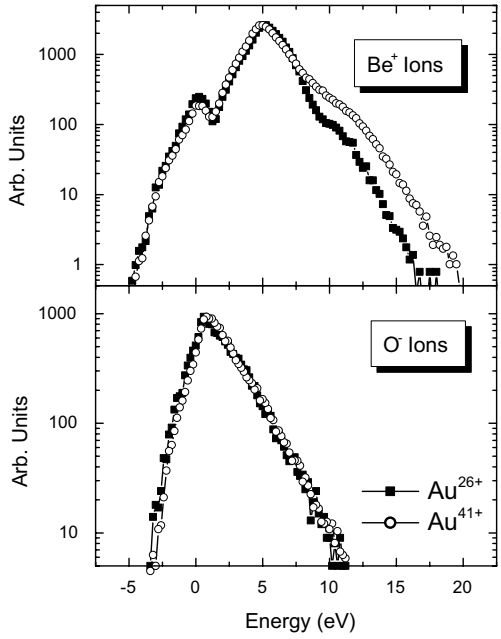

Fig. 3. Energy spectra of Be^+ and O^- ions sputtered from the BeO film by Au^{26+} and Au^{41+} beams at 1.8 MeV/u. Negative energy parts of the spectra result from a finite energy line width of the mass spectrometer.

1 eV and mainly because of residual magnetic fields the Be^+ energy spectrum is partially suppressed below a kinetic energy of about 5 eV. The influence of residual magnetic fields on the negative ion spectra was much weaker.

3. Results

The experimental angular distributions of Be^+ and O^- measured under irradiation of the BeO film by Au^{41+} ions and obtained by integration of energy spectra are displayed in Fig. 4. Since the incident angle α was varied during the measurements of the angular distribution and the sputtering yield increases for oblique impacts due to larger energy deposition in the surface layers, the experimentally observed yield behaves typically as $1/\cos\alpha$. On the other hand, the thermal emission of secondary particles should show the $\cos\beta$ dependence because of refraction at the surface binding potential. Applying both corrections we can define a corrected sputtering yield

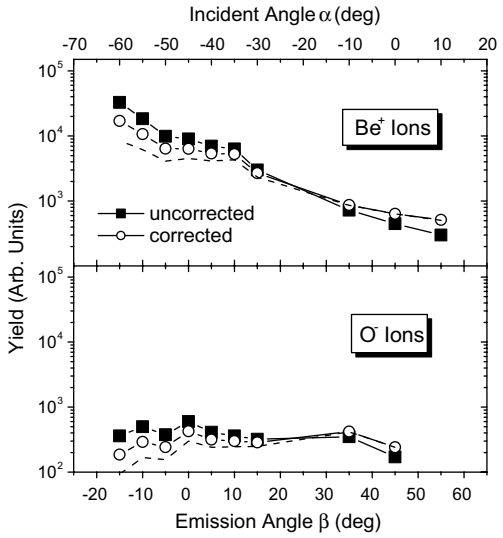

Fig. 4. Angular distribution of secondary ions sputtered from the BeO film by 1.8 MeV/u Au^{41+} ions. The correction of the data points is described in the text.

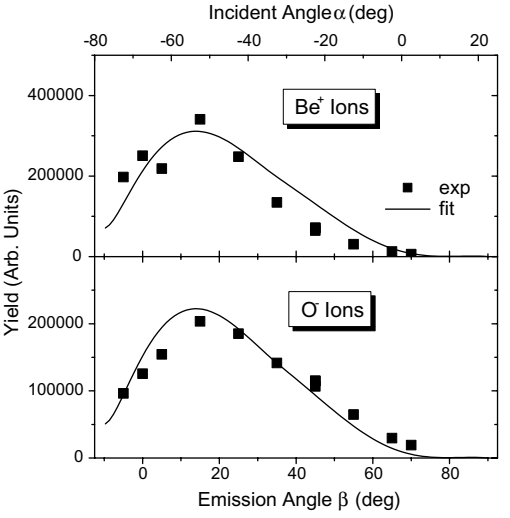

Fig. 5. Angular distributions of secondary ions sputtered from the BeO film by 2.5 keV Ar^+ ions. The curve describing nuclear sputtering was fitted to both data sets simultaneously.

$$Y_{\mathrm{corr}}(\alpha,\beta) = Y_{\mathrm{exp}}(\alpha,\beta)\ \cos\alpha/\cos\beta, \qquad (1)$$

which should be constant for a thermal emission that behaves linear with the deposited surface energy density. As shown in Fig. 4 the angular distribution of O^- ions agrees with this assumption quite well (curve with open circles), whereas the emission of Be^+ ions increases strongly for negative emission angles corresponding to the incident half-space. The dashed line without symbols represents in Fig. 4 the experimental data corrected for the stronger emission angle dependence of $\cos^{-2}\alpha$ observed in some experiments [17]. The results obtained for other ions imply that the discussed differences in angular distributions occur generally for positive and negative ions. This effect is illustrated quantitatively in Table 1 where the ratio of corrected yields for the sputtering emission angles $\beta = 0°$ and $\beta = 45°$ is compared for all ions measured.

For comparison the angular distributions obtained under nuclear sputtering conditions for 2.5 keV Ar^+ impact are presented in Fig. 5. The yields for both positive and negative ions show similar angular distributions with a maximum at the emission angle 15° (half-space opposite to the incident site). This maximum results from a partial conservation of the incident momentum during the nuclear collision cascade [5] and can roughly be described by a common fit curve proposed by [12] (see Fig. 5) for positive as well as negative ions. Thus, the significant rise of the Be^+ yield for negative incident angles in Fig. 4 is neither related to the apparatus nor to the surface properties of BeO.

Differences between negative and positive ions sputtered by the fast heavy ions can also be observed in energy spectra (see Fig. 3). High energy slopes are flatter for the positive ions than those for the negative ions. Energy spectra of the

Table 1
Experimental and corrected yield ratios $R_{\mathrm{corr}} = Y_{\mathrm{corr}}(\alpha = -45°, \beta = 0°)/Y_{\mathrm{corr}}(\alpha = 0°, \beta = 45°)$ for all measured ions (see Eq. (1)), averaged over the values obtained for both projectile charge states (Au^{26+} and Au^{41+})

Ions	Be^+	O^+	BeO_2^-	BeO^-	O^-
R_{exp}	26	27	3.5	3.3	3.7
R_{corr}	13	14	1.7	1.6	1.9

negative ionic compounds BeO^- and BeO_2^- show even steeper slopes than for O^-. Merely, in the energy spectra of positive ions, a strong high-energy component, enhanced for the Au^{41+} irradiation, can be observed (Fig. 3). The multi-peak structure, visible for positive ions at low emission energies, results probably from the residual magnetic field produced by an electron gun. In new measurements performed after removing the electron gun, we do not observe this structure anymore. In principle, one may interpret the flat high-energy slopes for positive ions in terms of an atomic emission temperature. A quantitative evaluation using fitted Maxwell–Boltzmann distributions, however, results in unreasonably high lattice temperatures even for the Au^{26+} case. Thus, we conclude that the 1+ charge state fraction of emitted ions is increasing with the sputtered-ion energy.

The energy integrated sputtering yields determined for the charge equilibrated Au^{41+} projectiles are by a factor 3.4 larger than those measured for the non-equilibrium charge state 26+. This increase of the ionic sputtering yield is roughly the same for all secondary ions and independent of the measuring geometry. Comparison of this increase to the theoretical stopping power ratio for both projectiles in BeO (factor 3.1 [6]) shows that the sputtering yield is a linear function of the stopping power. Contrary, the sputtering of LiF under irradiation of 1 MeV/u swift heavy ions [3] was found to be strongly non-linear: $Y \propto (\mathrm{d}E/\mathrm{d}x)^4$.

4. Discussion and conclusions

The differences in the angular distributions as well as in the energy spectra between positive and negative ions suggest different sputtering mechanisms under bombardment by swift heavy ions for both ion species. While the angular distribution of negative ions seems to be in agreement with the thermal spike model, a strong angular asymmetry as well as the high-energy contribution in energy spectra of positive ions provide a clear evidence for a non-equilibrium process taking place in the ion track. Contrary, the angular distributions measured within the nuclear regime show only small differences in the behavior of positive and negative ions. This suggests that resonant charge-exchange [7] at the BeO target surface as a reason for large differences observed in the electronic sputtering can be excluded. Moreover, since the resonant charge-exchange mechanism is specific for the ion species emitted, one should expect different angular distributions of Be^+ and O^+ ions in the electronic sputtering regime. This, however, was not observed in the experiment and therefore supports our conclusion additionally. Nevertheless, we cannot exclude an influence of the electronic energy deposition on the non-resonant charge-exchange mechanism.

Besides the angular distribution of positive ions, also the linear dependence of the ionic sputtering yield on the stopping power value cannot be explained within the thermal spike model that predicts a quadratic dependence [8,9].

The Coulomb explosion, resulting from the repulsive interaction among positive ions within the ion-track, can generally influence emission of positive and negative ions by means of the build-up of a positive ion-track potential [14]. However, we have not observed any energy shift of BeO Auger-decay lines during the incident of swift heavy ions [15]. This implies that the neutralization time of the ion-track in BeO should be smaller than the Auger-decay time of 10^{-14} s. Thus, the Coulomb explosion can be excluded as the energy transfer mechanism from the electronic excitation to the atomic system for the sputtering process, being on the time scale from 10^{-13} to 10^{-11} s. From the other hand, possible shock or pressure waves, created during the atomic energy transport outside from the center of the ion-track, can lead to some anisotropy of angular distribution. However, the influence of shock waves on the emission of positive and negative ions should be similar. Furthermore, one expects a maximum emission at the angle 45° with respect to the target surface for the normal incidence [16], which was not observed in our experiment.

An alternative description of the sputtering process provides the gas-flow model [10] assuming that the energy deposited in the ion-track exceeds the sublimation energy and leads to an adiabatic, directed gas flow outside the target. This model

could explain the strongly asymmetric angular distribution of emitted positive ions under an assumption that the jet-like angular distribution gets broader for oblique projectile impacts. In fact, such an effect was observed in the LiF experiments [3]. In contrast to those experiments, our total sputtering rate was much smaller and amounted only to about one to three atoms per projectile. This implies a relatively fast heat removal from the ion-track region and sputtering, consequently, only from the most upper surface layers of the BeO target. The restriction to the very surface leads to an additional broadening of the angular distribution. The gas-flow model, despite a very simple physical picture, agrees with the results of much more sophisticated, molecular-dynamics (MD) calculations. According to the MD studies performed for the solid argon target [9] under assumption of the Lennard–Jones interaction, a flow of atoms along the ion-track towards the target surface could be observed. This caused much stronger angular dependence of sputtered particles than that expected for the thermal spike model. Recently, an improved MD simulation including the initial ionization of the cylindrical ion-track has been presented [11]. It could be shown that the sputtering process has two components: a prompt component from the track core providing more energetic ejectiles and a component from a larger, equilibrated region contributing slower particles. Taking into account that the ion track initially remains in a highly ionized plasma state [13] and neutralization of primary positive ions or creation of negative ions at the target surface is strongly suppressed due to relatively high kinetic energies of positive ions, the following scenario of the sputtering process can be suggested: the positive ions should preferentially be emitted as constituents of the plasma flow during the first stages of the ion-track evolution, whereas the negative ions could be created mostly at a later time scale when the thermal equilibrium occurs in a larger target region.

Consequently, the discussion above leads to the conclusion that the study of emission of positive and negative ions might enable an access to sputtering processes at different time scales. However, further detailed experimental investigations and more sophisticated theoretical studies including the charge-exchange phenomena are necessary.

References

[1] C. Dufour et al., J. Phys.: Condens. Matter 5 (1993) 4573.
[2] M. Toulemonde, Ch. Dufour, A. Meftah, E. Paumier, Nucl. Instr. and Meth. B 166–167 (2000) 903.
[3] M. Toulemonde, W. Assmann, C. Trautmann, F. Grüner, Phys. Rev. Lett. 88 (2002) 057602.
[4] G. Schiwietz, K. Czerski, M. Roth, F. Staufenbiel, E. Luderer, P.L. Grande, Nucl. Instr. and Meth. B 193 (2002) 705.
[5] H.E. Roosendaal, J.B. Sanders, Radiat. Eff. 52 (1980) 137.
[6] G. Schiwietz, P.L. Grande, code CasP. Available from www.hmi.de/people/schiwietz/casp.html.
[7] M.L. Yu, N.D. Lang, Nucl. Instr. and Meth. B 14 (1986) 403.
[8] K.M. Gibs, W.L. Brown, R.E. Johnson, Phys. Rev. B 38 (1988) 11001.
[9] E.M. Bringa, R.E. Johnson, L. Dutkiewicz, Nucl. Instr. and Meth. B 152 (1999) 267.
[10] H.M. Urbassek, J. Michl, Nucl. Instr. and Meth. B 22 (1987) 480.
[11] E.M. Bringa, Nucl. Instr. and Meth. B 209 (2003) 1.
[12] J.-F. Hennequin, J. Phys. 29 (1968) 957.
[13] R.H. Ritchie, C. Claussen, Nucl. Instr. and Meth. B 198 (1982) 133.
[14] G. Schiwietz, P.L. Grande, B. Skogwall, J.P. Biersack, R. Köhrbrück, K. Sommer, A. Schmoldt, P. Goppelt, I. Kádár, S. Ricz, U. Stettner, Phys. Rev. Lett. 69 (1992) 628.
[15] K.Czerski, G. Schiwietz, M. Roth, F. Satufenbiel, P.L. Grande, ISL HMI Annual Report 2003, p. 54.
[16] R.E. Johnson, B.U.R. Sundquist, A. Hedin, D. Fenyö, Phys. Rev. B 40 (1988) 49.
[17] M. Toulemonde, W. Assmann, C. Trautmann, F. Grüner, H.D. Mieskes, H. Kucal, Z.G. Wang, Nucl. Instr. and Meth. 212 (2003) 346.